Journal of Molecular Structure 1154 (2018) 619–625

Contents lists available at ScienceDirect

Journal of Molecular Structure

journal homepage: http://www.elsevier.com/locate/molstruc

Synthesis, spectra and X-ray crystallography of dipyridin-2-ylmethanone oxime and its $CuX_2(oxime)_2$ complexes: Thermal, Hirshfeld surface and DFT analysis

Ismail Warad [a, *], Muneer Abdoh [b, **], Anas Al Ali [a], Naveen Shivalingegowda [c], Karthik Kumara [d], Abdelkader Zarrouk [e], Neartur Krishnappagowda Lokanath [d]

[a] Department of Chemistry, Science College, An-Najah National University, P.O. Box 7, Nablus, Palestine
[b] Department of Physics, Science College, An-Najah National University, P.O. Box 7, Nablus, Palestine
[c] Department of Basic Sciences, School of Engineering and Technology, Jain University, Bangalore, 562 112, India
[d] Department of Studies in Physics, University of Mysore, Manasagangotri, Mysuru, 570 006, India
[e] LCAE-URAC18, Facult_e des Sciences d'Oujda, Universit_e Mohammed Premier, BP 4808, 60046, Oujda, Morocco

ARTICLE INFO

Article history:
Received 31 July 2017
Received in revised form
24 October 2017
Accepted 24 October 2017
Available online 27 October 2017

Keywords:
Copper(II) complex
Oxime
FT-IR spectrum
DFT
XRD

ABSTRACT

Dipyridin-2-ylmethanone oxime ($C_{11}H_9N_3O$), was prepared using di-2-pyridyl ketone. The oxime ligand and its neutral CuX_2 (oxime)$_2$ (X = Cl or Br) complexes have been identified with the aid of several spectroscopic techniques such as: IR, EI-MS, EA, UV–visible, TG, ^{1}H-NMR and finally the structure of the free oxime ligand was confirmed by X-ray diffraction studies. The oxime crystallizes in the monoclinic space group $P2_1/c$, with cell parameters $a = 8.8811$ (8) Å, $b = 10.6362$ (8) Å, $c = 11.2050$ (8) Å, $\beta = 109.085$ (4) °, $V = 1000.26$ (14) Å^3 and $Z = 4$. The molecular conformation is stabilized by a strong intramolecular O–H···N hydrogen bonding between the hydroxyl group of the oxime moiety and the nitrogen of the pyridine ring.

Since the oxime structure was solved by XRD, the ligand structure parameters like bond length and angles were compared to the DFT computed one, the UV–visible to TD-SCF and Hirshfeld surface to MEP analysis.

1. Introduction

Synthesis of oximes from carbonyl functionalities is an important reaction in organic synthesis and medical applications [1]. Oximes are prepared classically by refluxing an alcoholic solution of a carbonyl compound with hydroxylamine hydrochloride in basic media [2]. Oximes are stable crystalline materials that find applications in many chemical fields such as, purification and protection of carbonyl compounds [1,2], conversions into nitro [3], nitriles [4], nitrones [5], amines [6], and synthesis of azaheterocycles [7]. They serve as intermediates for the synthesis of amides through the Beckmann rearrangement [8,9] and also as herbicides and fungicides [10]. In inorganic chemistry, oxime (C=N–OH) and oxidate (C=N–O$^-$) groups can bind metal ions in a variety of coordination modes and are thus ideal candidates for reactivity chemistry [11]. Oximes act as a versatile neutral polydentate ligand especially if pyridine derivatives were incorporated in their backbone [12]. The activation of oximes though coordination reaction with metal ions is also becoming a fruitful research area [13,14]. For the same reason the synthesis of a polydentate oxime chelate ligand is still a challenge and has attracted many coordination chemists [13–16]. In view of this, dipyridin-2-ylmethanone oxime and its CuX_2 (oxime)$_2$ (X = Cl or Br) were synthesized and spectroscopically characterized by FT-IR, EI-MS, UV–visible, TG, NMR techniques and finally the structure of the oxime was confirmed by X-ray diffraction analysis then computed by DFT calculations.

2. Experimental

2.1. Instruments

Solution UV–visible spectra were measured by using a TU-1901 double-beam UV–visible spectrophotometer. The IR

* Corresponding author.
** Corresponding author.
E-mail address: warad@najah.edu (I. Warad).

https://doi.org/10.1016/j.molstruc.2017.10.087
0022-2860/

Table 1
Crystal data and structure refinement.

CCDC number	1401887
Empirical formula	$C_{11}H_9N_3O$
Formula weight	199.21
Temperature	293 (2) K
Wavelength	1.54178 Å
Crystal system, space group	Monoclinic, $P2_1/C$
Unit cell dimensions	$a = 8.8811$ (8) Å $b = 10.6362$ (8) Å $c = 11.2050$ (8) Å $\beta = 109.085$ (4)°
Volume	1000.26 (14) $Å^3$
Z, Calculated density	4, 1.323 Mg/m^3
Absorption coefficient	0.727 mm^{-1}
$F_{(000)}$	416
Crystal size	0.3 × 0.27 × 0.25 mm
Theta range for data collection	5.90° to 64.06°
Limiting indices	$-9 \leq h \leq 10$, $-11 \leq k \leq 12$, $-13 \leq l \leq 13$
Reflections collected/unique	4799/1538 [R (int) = 0.0319]
Refinement method	Full-matrix least-squares on F^2
Data/restraints/parameters	1538/0/137
Goodness-of-fit on F^2	1.175
Final R indices [$I > 2\sigma(I)$]	$R1 = 0.0477$, w$R2 = 0.1234$
R indices (all data)	$R1 = 0.0594$, w$R2 = 0.1405$
Extinction coefficient	0.037 (4)
Largest diff. peak and hole	0.319 and −0.321 e. $Å^{-3}$

spectra for solid samples were recorded using Perkin Elmer Spectrum 1000 FT-IR Spectrometer. High-resolution (400 MHz) ^1H NMR spectrum was recorded on a Bruker Advance II 400HR spectrometer at 293 K, with 5 mm PABBO BB-1H TUBES, using $CDCl_3$ as a solvent and TMS as internal standard (chemical shift in δ ppm). EI-MS data was obtained on a 711A (8 kV) Finnigan. TG/DTA spectrum was measured by using a TGA-7 PerkinElmer thermogravimetric analyzer.

2.2. Materials and methods

All the reagents [dipyridin-2-ylmethanone, hydroxylamine hydrochloride and sodium acetate, copper (II)bromide] and solvents [ethanol and methanol] used in this study were of analytical grade and purchased from Sigma–Aldrich and used as received. The purity of the compounds was confirmed by thin-layer chromatography using Merck silica gel 60 F254 coated aluminum plates.

2.2.1. Procedure for the preparation of Dipyridin-2-ylmethanone oxime

A mixture of dipyridin-2-ylmethanone (1 mmol), hydroxylamine hydrochloride (1.2 mmol), and sodium acetate (1.2 mmol) was refluxed for 4 h in 50 mL ethanol solvent. The solution was concentrated down to approx. 5 mL, then water added to it when product precipitated out from the solution. The precipitate formed was filtered off and recrystallized from methanol. Yield 70%, m.p. 105–110 °C. MS m/z = 199.0 (199.2 theoretical). Calcd. for $C_{11}H_9N_2O$: C, 66.32; H, 4.55; N, 21.09. Found: C, 66.45; H, 4.31; N, 20.85.

2.2.2. Synthesis of the complexes

A solution of oxime ligand (0.10 mmol) dissolved in 10 mL of EtOH was added to (0.05 mmol) of $CuX_2.2H_2O$ dissolved in 5 mL of EtOH. The occurrence of the complexation process was confirmed by color changes. The Cu(II) complex precipitant was collected by solvent evaporation (Yield ~ 85%).

2.2.2.1. Complex 1. MS m/z = 531.0 [M^+] calc. MS = 532.9. Anal. Calcd for $C_{22}H_{18}Cl_2CuN_6O_2$: C, 49.59; H, 3.40; N, 15.77, found: C, 49.46; H, 3.38; N, 15.67%. Conductivity in water: 80 (μS/cm).

2.2.2.2. Complex 2. MS m/z = 620.0 [M^+] calc. MS = 621.77. Anal.

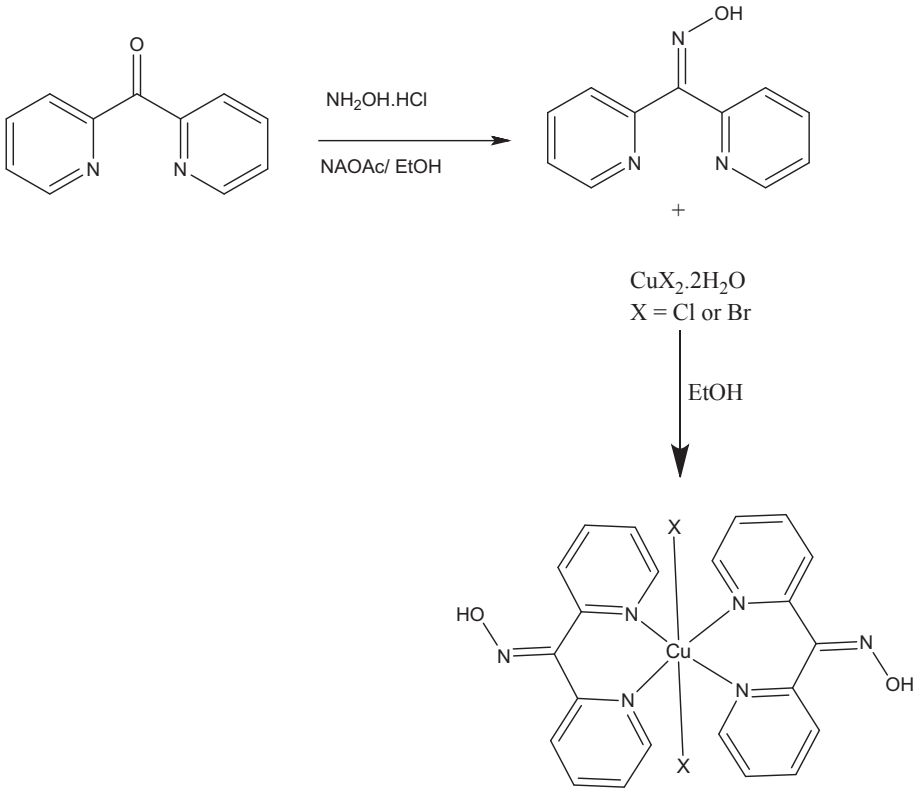

Scheme 1. Synthesis of oxime ligand and its complexes.

Table 2
Hydrogen-bond geometry (Å, °).

D—H···*A*	*D*—H	H···*A*	*D*···*A*	*D*—H···*A*
O—H···N	0.82	2.03	2.7971	155
C—H···N	0.93	2.69	3.292	123
C—H···O	0.93	2.71	3.378	129

Calcd for $C_{22}H_{18}Br_2CuN_6O_2$: C, 42.50; H, 2.92; N, 13.52. Found: C, 42.33; H, 2.89; N, 13.42%. Conductivity in water: 65 (μS/cm).

2.2.2.3. Single crystal X-ray diffraction. Single crystals suitable for X-ray diffraction study were obtained by a slow evaporation technique using ethanol as a solvent. A white coloured prism shaped single crystal of dimensions 0.3 × 0.27 × 0.25 mm of the oxime was chosen for an X-ray diffraction study. The X-ray intensity data were collected at a temperature of 293 K on a Bruker Proteum2 CCD diffractometer equipped with an X-ray generator operating at 45 kV and 10 mA, using CuK_α radiation of wavelength 1.54178 Å. Data were collected for 24 frames per set with different settings of φ (0° and 90°), keeping the scan width of 0.5°, exposure time of 2 s, the sample to detector distance of 45.10 mm and 2θ value at 46.6°. A complete data set was processed using *SAINT PLUS* [17]. The structure was solved by direct methods and refined by full-matrix least squares method on F^2 using *SHELXS* and *SHELXL* programs [18]. All the non-hydrogen atoms were revealed in the first difference Fourier map itself. All the hydrogen atoms were positioned geometrically (C—H = 0.93 Å, O—H = 0.82 Å) and refined using a riding model with $U_{iso}(H) = 1.2\ U_{eq}$ and $1.5\ U_{eq}$ (O). After ten cycles of refinement, the final difference Fourier map showed peaks of no chemical significance and the residuals refined to 0.0477. The geometrical calculations were carried out using the program *PLATON* [19]. The molecular and packing diagrams were generated using the software *MERCURY* [20]. The details of the crystal structure and data refinement are given in Table 1.

2.2.3. Computational details

Gaussian 09 program was used for the calculations [21,22]. B3LYP method and 6-31G (d,p) basis set was performed. Hirshfeld surface analysis was performed using the CRYSTAL EXPLORER 3.1 software [23].

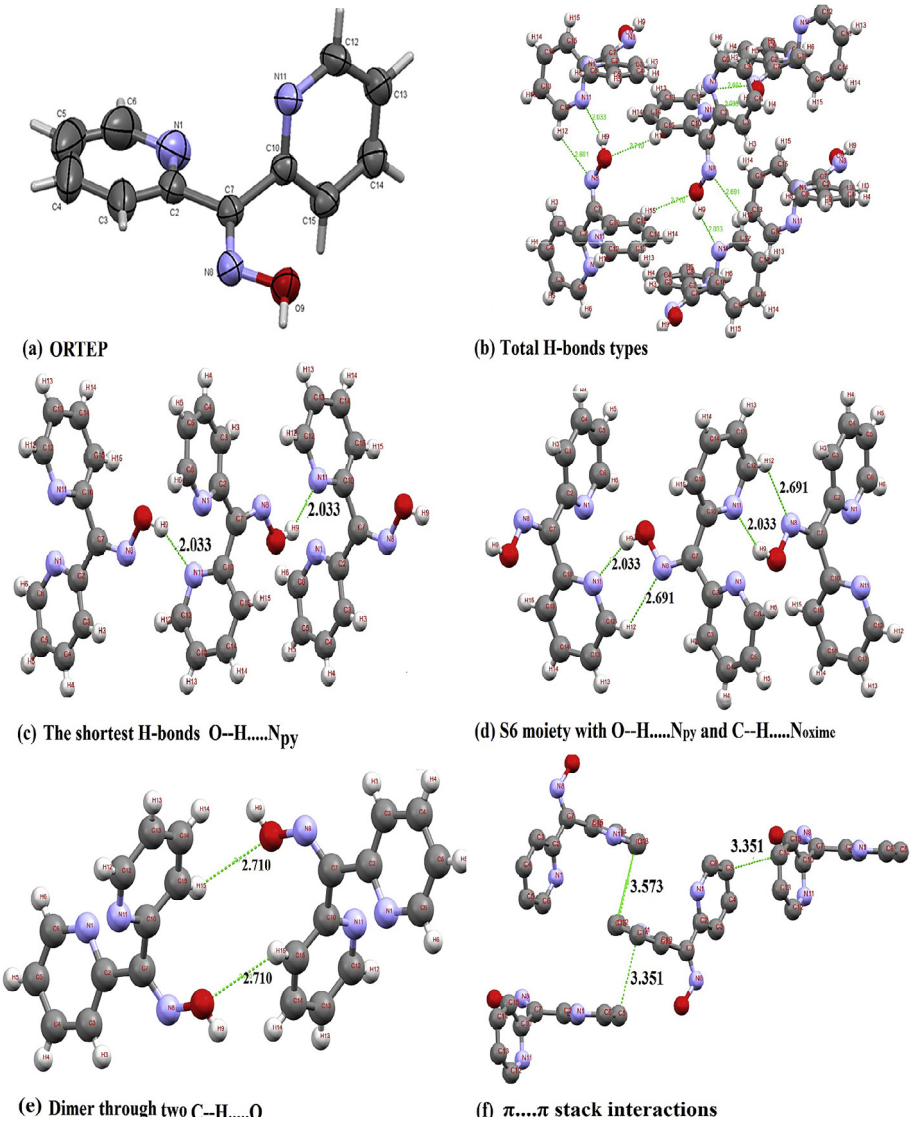

Fig. 1. (a) ORTEP diagram of the molecule with thermal ellipsoids drawn at 50% probability and (b–f) Packing of the molecules together with all the intermolecular force types.

Table 3
Experimental and DFT bond lengths and angles for desired oxime.

Bond type		Bond length [Å]		Angle type			Angle value (°)	
		DFT	XRD				DFT	XRD
N1	C2	1.3429	1.339 (2)	C2	N1	C6	117.81	116.3 (2)
N1	C9	1.3358	1.348 (4)	O9	N8	C7	113.23	113.5 (1)
C2	C3	1.4031	1.383 (3)	C10	N11	C12	117.7	117.0 (1)
C2	C11	1.4903	1.482 (3)	N1	C2	C3	122.76	123.4 (2)
C3	C5	1.3909	1.376 (5)	N1	C2	C7	116.03	115.3 (2)
C5	C7	1.3953	1.356 (5)	C3	C2	C7	121.2	121.3 (2)
C7	C9	1.3955	1.374 (5)	C2	C3	C4	118.64	118.2 (2)
C11	N12	1.2881	1.282 (2)	C3	C4	C5	118.92	119.7 (3)
C11	C15	1.4963	1.497 (2)	C4	C5	C6	118.1	118.7 (3)
N12	O13	1.4009	1.392 (2)	N1	C6	C5	123.77	123.6 (3)
O13	H14	0.9703	0.82 (2)	N8	C7	C2	115.48	116.2 (1)
C15	N16	1.3421	1.34 (2)	N8	C7	C10	125.75	124.6 (1)
C15	C23	1.3996	1.377 (2)	C2	C7	C10	118.78	119.3 (1)
N16	C17	1.3355	1.341 (2)	N11	C10	C7	115.33	115.9 (1)
C17	C19	1.3962	1.374 (5)	N11	C10	C15	123	122.8 (1)
C19	C21	1.3939	1.368 (3)	C7	C10	C15	121.67	121.3 (1)
C21	C23	1.3926	1.378 (3)	N11	C12	C13	123.7	123.6 (2)
				C12	C13	C14	118.19	118.6 (2)
				C13	C14	C15	118.84	119.0 (2)
				C10	C15	C14	118.56	119.0 (2)

3. Results and discussion

3.1. Synthesis

The reaction scheme for the synthesis of desired oxime and its complexes are depicted in Scheme 1. Dipyridin-2-ylmethanone oxime product was obtained in a good yield by condensation of dipyridin-2-ylmethanone with hydroxylamine hydrochloride in basic medium using ethanol solvent under refluxing condition.

Water soluble neutral complex **1** and **2** were made available by reacting two equivalent amounts of oxime ligand with hydride CuX_2 dissolved in ethanol. The desired complexes have been isolated as halide salts in very good yields. The color change from light brown to green or to blue indicated the formation of complex **1** and complex **2**, respectively. Since we did not solve the X-ray structure of any of the complexes, the neutral nature was supported by their conductivity, solubility, elemental analysis, UV–vis. spectral method and DFT calculation, as seen in Scheme 1.

3.2. Crystal and structure optimization

The list of bond lengths and angles of the non-hydrogen atoms are given in Table 2. Fig. 1 represents the ORTEP and packing system of the oxime molecule with thermal ellipsoids drawn at 50% probability.

The molecule is non-planar; the two aromatic rings are bridged *via* the N-pyridine of oxime ligand. The bond lengths and angles are normal in their values, the molecular conformation is characterized by a dihedral angle of 83.06 (11)° between the mean planes of the two aromatic rings indicating that they are nearly orthogonal to each other, as seen in Fig. 1, the collected result in this work is consisted with same reported structural data [24]. The rotation of the aromatic rings is characterized by the torsion angles relative to the oxime plane. The molecular conformation is stabilized by a main strong intramolecular O–H···N hydrogen bonding between the hydroxyl group of the oxime moiety and the nitrogen of the pyridine ring. The hydrogen bond (H···N) in O9–H9···N11 has a length of 2.03 Å and an angle of 155° which links the molecule to form a chain like structure, as seen in Table 2 and Fig. 1b–c. The packing of the molecules reflected many short contacts between molecule and neighbor molecule, as seen in Fig. 1b. Two S6 moiety were formed around each molecule in the lattice by O–H … N_{py} and new C_{py}–H … N_{oxime} (2.69 Å length) H-bonds, as seen in Fig. 1d. Each molecule in the lattice was dimerized with its neighbor through two C_{py}–H…O (2.71 Å length) H-bonds, as seen in Fig. 1e. Three π …. π stack interactions per molecule have a length of 3.35 and 3.57 Å were detected as in Fig. 1e. These hydrogen bonded chains stabilized the lattice into the 3D network.

The crystal data (cif files) for desired oxime was used to compare the bond lengths and angles structure parameters with the theoretical DFT result, as seen in Table 3. The plot of the X-ray experimental bond lengths against computed bond lengths (Fig. 2a) and experimental angles against DFT theoretical (Fig. 2b) reflected an excellent matching with $R^2 = 0.977$ and $R^2 = 0.961$ correlation coefficient respectively.

3.3. Hirshfeld surface and MEP analysis

Hirshfeld surface (HAS) and MEP analysis was computed using CIF file of the desired oxime. HAS comprising of d_{norm} surface and MEP electrostatic potentials were recorded, as in Fig. 3a. The d_{norm} reflected two big-red spots on the surface of each molecule which is consistent with the presence of a hydrogen bond. Two types of O–H …. Npy H-bonds were detected crucially stabilized the molecular crystal structure [24–27].

In the MEP map the nucleophilic (N_{py}) and electrophilic (O–H) positions as a preferred position for the H-bonding formation (Fig. 3b). The blue region in the structure indicated the e-poor (electrophilic) functional group while the red region is due to the e-rich nucleophilic functional group, for that MEP indicated that the two nitrogen atoms of the pyridine rings act as bi-dentate ligand, while the = N–*O*–H side is blocked and not suitable for metal ion coordination since it is busy with O–-H … N_{py} hydrogen bonding.

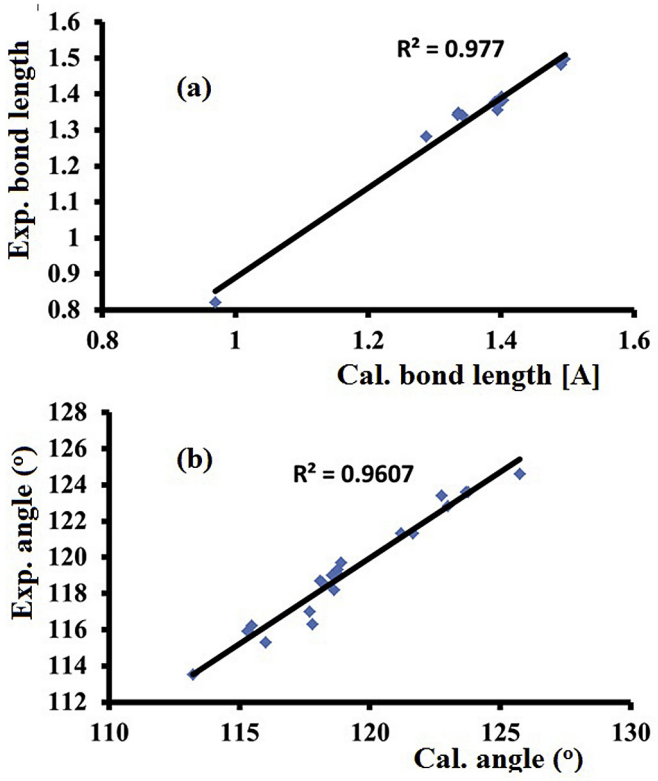

Fig. 2. Graphical correlation of: a) DFT vs. experimental bond lengths (Å) and (b) DFT *vs.* experimental angles (°).

The protons of H–C belong to pyridine groups are green in color which reflected their electrophilicity natural. These observations are consistent with HSA results.

3.4. ^{1}H NMR analysis of the oxime

The ^{1}H NMR spectrum of the crystal structure was very simple; only two types of signals were recorded. ^{1}H NMR spectrum showed sharp singlet at δ 9.7 ppm due to = NOH protons. The four pyridle protons resonated as a multiplet in the region of δ 7.3–8.6 ppm.

3.5. UV–Vis analysis

UV–Vis. spectrum of the oxime and its complexes were recorded in ethanol at room temperature as shown in Fig. 4. The absorption bands of the oxime are TD-DFT/B3LYP/6-311 (d,p) were computed in gaseous state and ethanol solvent. From the graph, it was observed that the oxime showed experimentally two absorption peaks at λ_{max} = 225 and 275 nm attributed to the π-π^* transition. Hence, the material may be useful for optoelectronic applications (Fig. 4a). The time-dependent DFT UV–Vis. spectrum absorption maximum was found with mean broad maxima at λ_{max} = 250 nm in both vacuum and ethanol solvent (Fig. 4b), which reflected no solvent effect was detected.

The oxime-complexes **1** and **2** revealed two signals in the UV area similar to the free oxime; DMSO-d_6 electron transition broad band in the visible area at λ_{max} = 615 nm (complex **2**) and λ_{max} = 660 nm (complex **1**) were recorded, as in Fig. 4c.

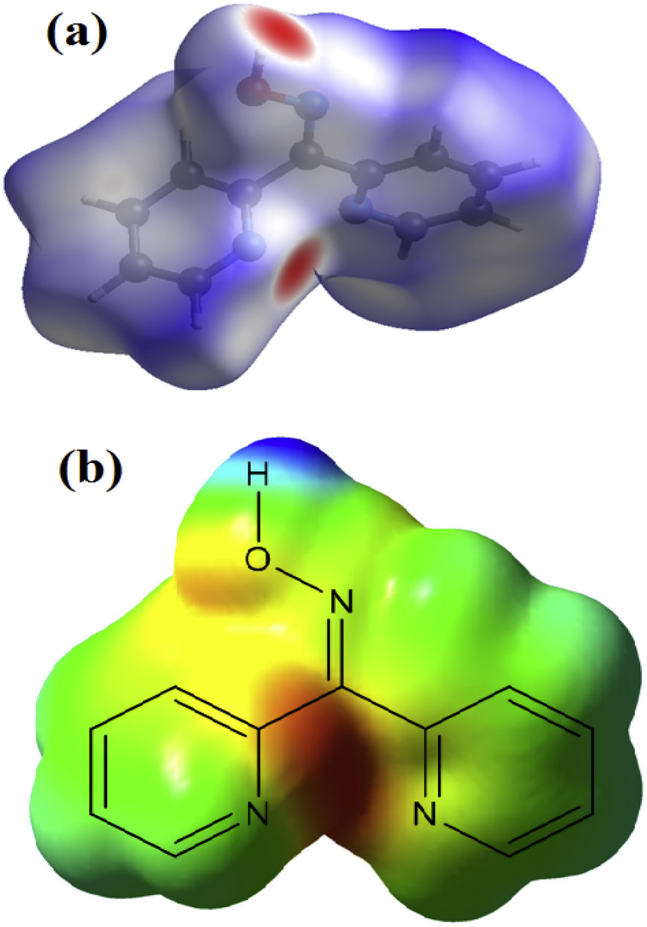

Fig. 3. d_{norm} (a) and MEP map (b) of the oxime.

3.6. FT-IR spectral analysis

The FT-IR spectrum of the solid powder of oxime is shown in Fig. 5a. IR spectra showed several modes of vibrations; the main absorption vibration bands only were cited. The vibration bands at 3165 cm^{-1} cited to the hydroxyl function group, vibration bands at 3020-2850 cm^{-1} due to C–H groups stretching vibration of pyridine. The absorption peak at 1680 cm^{-1} is due to the stretching vibration that corresponds to C=N group. The absorption at 960 cm^{-1} is characteristic of N–O stretching vibration in oxime moiety. The powder of the complexes revealed similar IR behavior, complex **1** showed no water broad peak vibrations of $\nu_{(O-H)}$ at ~ 3400 cm^{-1} indicating the absence of water molecule in the

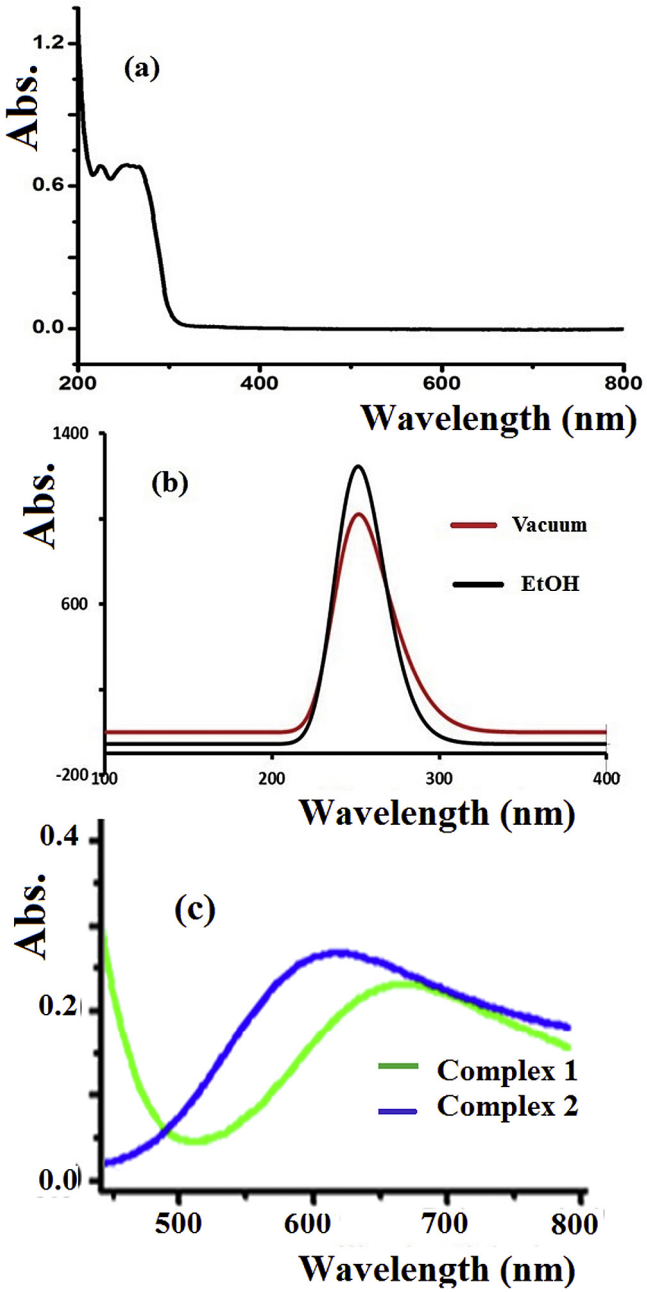

Fig. 4. (a) UV–Vis spectrum of 1 × 10^{-5} M oxime in EtOH at RT, (b) TD-DFT/B3LYP/6-311 (d,p) in gaseous state and ethanol solvent, (c) 1 × 10^{-4} M of complex **1** and **2** dissolved in ethanol at RT.

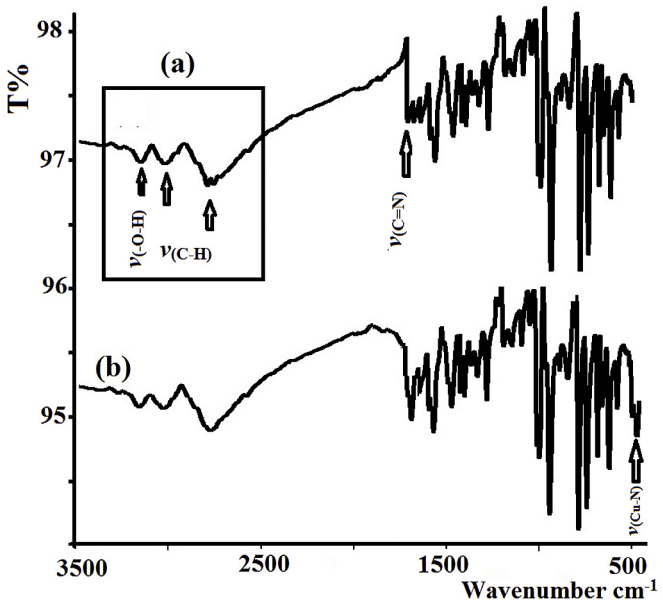

Fig. 5. The FT-IR spectra: (a) for the free oxime ligand and (b) complex **1**.

crystal lattice of molecule. The IR of the free oxime and complex **1** are very similar compared to the free ligand, the existence of a sharp peak at ~500 cm^{-1} for the complex (not the free oxime) indicated the N–Cu(II) bonds formation (Fig. 5b).

3.7. Thermal analysis

To understand the thermal properties, TG analyses of the free oxime and its complexes have been performed individually under an open atmosphere in the range of 0–1000 °C with heating rate of 10 °C/min (Fig. 6). The TG-curve showed that the oxime exhibits a remarkable thermal stability at about 100 °C. The oxime decomposed mainly in one broad step, a typical decomposition started from ~105 °C and end at ~180 °C, with weight loss ~99%, no intermediate decomposition steps were detected (Fig. 6a).

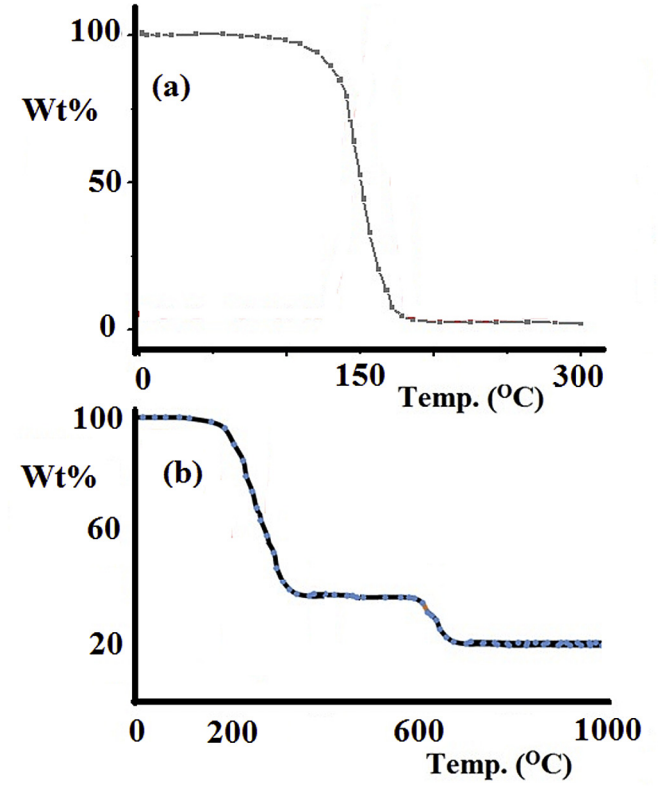

Fig. 6. TG thermal curves of the free oxime (a) and complex **2** (b).

The TG spectrum of complex **2** illustrated mainly two steps of weight loss. First step was losing of both oxime ligands from 180 °C and end at 370 °C losing around 64% of weigh to form $CuBr_2$. The second decomposition stage started from 560 °C to 650 °C which lead to the removal of bromide from $CuBr_2$ and reacting with O_2 (open atmosphere) to form copper oxide product, 18% final (Fig. 6b).

4. Conclusions

The dipyridin-2-ylmethanone oxime and CuX_2 (oxime)$_2$ complexes were synthesized and characterized by means of various spectroscopic tools like: IR, UV–visible, MS, EA, TG, ^{1}H-NMR and finally the structure of the free oxime was confirmed by X-ray diffraction studies. DFT/B3LYP theoretical optimization of the oxime matched with experimental XRD structural result. The Hirshfeld surface and MEP analyses are consistent with the presence of strong O–H···N hydrogen bond formation as seen in the XRD packing analysis. The theoretical TD-SCF and experimental UV–visible showed no solvent effect on the electron transition in the oxime. TG-result revealed the oxime ligand and its complex **2** are decomposed completely through different thermal decomposition mechanisms.

Acknowledgments

The authors are grateful to the Institution of Excellence, Vijnana Bhavana, University of Mysore, India, for providing the single-crystal X-ray diffractometer facility. Prof. Warad would like to thank An-Najah University for its financial coverage of his recent scientific visit.

References

[1] Y.Q. Xie, Z.L. Huang, H.D. Yan, J. Li, L. Y.Ye, L.M. Che, S. Tu, Design, synthesis, and biological activity of oxime ether strobilurin derivatives containing indole moiety as novel fungicide, Chem. Biol. Drug. Des. 85 (2015) 743–755.
[2] T.W. Greene, P.G.M. Wuts, Protective Groups in Organic Synthesis, third ed., Wiley, Toronto, 1999, pp. 355–358.
[3] F.P. Ballistreri, E. Barbuzzi, G.A. Tomaselli, R.M. Toscano, Useful oxidation procedure of oximes to nitro compounds with Benz-Mo in acetonitrile, Synlett 11 (1996) 1093–1094.
[4] S.K. Dewan, R. Singh, A. Kumar, One pot synthesis of nitriles from aldehydes and hydroxylamine hydrochloride using sodium sulphate (anhyd) and sodium bicarbonate in dry media under microwave irradiation, Arkivoc 2 (2006) 41–44.
[5] P.A. Smith, S.E. Gloyer, Oxidation of dibenzylhydroxylamines to nitrones. Effects of structure and oxidizing agent on composition of the products, J. Org. Chem. 40 (1975) 2508–2512.
[6] S. Negi, M. Matsukura, M. Mizuno, K. Miyake, N. Minami, Synthesis of (2R)-1-(4-Chloro-2-pyridyl)-2-(2-pyridyl) ethylamine: a selective oxime reduction and crystallization-induced asymmetric transformation, Synthesis 8 (1996) 991–996.
[7] K. Narasaka, Synthesis of azaheterocycles from oxime derivatives, Pure Appl. Chem. 75 (2003) 19–28.
[8] C. Ramalingan, Y.T. Park, Mercury-catalyzed rearrangement of ketoximes into amides and lactams in acetonitrile, J. Org. Chem. 72 (2007) 4536–4538.
[9] Y. Furuya, K. Ishihara, H. Yamamoto, Cyanuric chloride as a mild and active Beckmann rearrangement catalyst, J. Am. Chem. Soc. 127 (2005) 11240–11241.
[10] B.A. Song, X.H. Liu, S. Yang, D.Y. Hu, L.H. Jin, Y.T. Zhang, Recent advance in synthesis and biological activity of oxime derivatives, Chin. J. Org. Chem. 25 (2005) 507–525.
[11] D. Garnovskii, V.Y. Kukushkin, Metal-mediated reactions of oximes, Russ. Chem. Rev. 75 (2006) 111–124.
[12] V. Duros, H. Sartzi, S. Teat, Y. Sanakis, O. Roubeau, S. Perlepes, Tris {2, 4-bis (2-pyridyl)-1, 3, 5-triazapentanedienato} manganese (III), a complex derived from a unique metal ion-assisted transformation of pyridine-2-amidoxime,

Inorg. Chem. Comm. 50 (2014) 117–121.
[13] G. Ramazan, E. Oktay, D. Nefise, One-pot synthesis of a new 2-substituted 1, 2, 3-triazole 1-oxide derivative from dipyridyl ketone and iso-nitrosoacetophenone hydrazone: nickel (II) complex, DNA binding and cleavage properties, Bioorg. Chem. 71 (2017) 325–334.
[14] O.A. Adebayo, K.A. Abboud, G. Christou, New mixed-valence Mn II 4 Mn IV clusters from an unusual ligand transformation, Polyhedron 122 (2017) 71–78.
[15] T.C. Stoumpos, R. Inglis, O. Roubeau, H. Sartzi, A.A. Kitos, C.J. Milios, G. Aromí, A.J. Tasiopoulos, V. Nastopoulos, E.K. Brechin, S.P. Perlepes, Rare oxidation-state combinations and unusual structural motifs in hexanuclear Mn complexes using 2-pyridyloximate ligands, Inorg. Chem. 49 (2010) 4388–4390.
[16] B.L. Westcott, G. Crundwell, M. Remesic, K. Knopf, K. Chandler, J. McMaster, E.S. Davies, Crystal structure and magnetic properties of di-copper and di-zinc complexes with di-2-pyridyl ketone oxime, Inorg. Chem. Commun. 74 (2016) 79–81.
[17] Bruker, SAINT PLUS, Bruker AXS Inc., Madison, Wisconsin, USA, 2012.
[18] G.M. Sheldrick, A short history of SHELX, Acta. Cryst. A64 (2008) 112–122.
[19] A.L. Spek, PLATON, an integrated tool for the analysis of the results of a single crystal structure determination, Acta. Cryst. A46 (C34) (1990).
[20] C.F. Macrae, I.J. Bruno, J.A. Chisholm, P.R. Edgington, P. McCabe, E. Pidcock, L. Rodriguez-Monge, R. Taylor, J. van de Streek, P.A. Wood, Mercury CSD 2.0–new features for the visualization and investigation of crystal structures, J. Appl. Cryst. 41 (2008) 466–470.
[21] M. Frisch, G.W. Trucks, H. Schlegel, G.E. Scuseria, M.A. Robb, J.R. Cheeseman, J.M. Millam, Gaussian 03, Revision c. 02, Gaussian. Inc., Wallingford, CT, 2004, p. 4.
[22] R. Ennington, T. Keith, J. Millam, Semichem Inc. Shawnee Mission KS, GaussView, Version, 5, 2009.
[23] S.K. Wolff, D.J. Grimwood, J.J. McKinnon, D. Jayatilaka, M.A. Spackman, Crystal explorer 2.1, University of Western Australia, Perth (, 2007.
[24] F. Hintermaier, W. Beck, K. Polborn, CCDC 199719: bis(2-Pyridyl)ketone oxime, CSD Communication, 2014, https://doi.org/10.5517/cc6ptk7.
[25] I. Warad, A. Barakat, Synthesis, physicochemical analysis of two new hemi-labile ether-phosphine ligands and their first stable bis-ether-phosphine/cobalt(II) tetrahedral complexes, J. Mol. Struct. 1134 (2017) 17–24.
[26] I. Warad, Y. Al-Demeri, M. Al-Nuri, S. Shahwan, M. Abdoh, Sh Naveen, N.K. Lokanath, M.S. Mubarak, T. Ben Hadda, Y.N. Mabkhot, Crystal structure, Hirshfeld surface, physicochemical, thermal and DFT studies of (N1E, N2E)-N1,N2-bis((5-bromothiophen-2-yl)methylene) ethane-1,2-diamine N2S2 ligand and its [CuBr(N2S2)]Br complex, J. Mol. Struct. 1142 (2017) 217–225.
[27] I. Warad, F.F. Awwadi, M. Daqqa, A. Al Ali, T.S. Ababneh, T.M.A. AlShboul, T.M.A. Jazzazi, F. Al-Rimawi, T. Ben Hadda, Y.N. Mabkhot, New isomeric Cu(NO_2-phen)$_2$Br]Br complexes: crystal structure, Hirschfeld surface, physicochemical, solvatochromism, thermal, computational and DNA-binding analysis, J. Photochem. Photobiol. B Biol. 171 (2017) 9–19.